Supporting Information

Zhai et al. 10.1073/pnas.1418918112

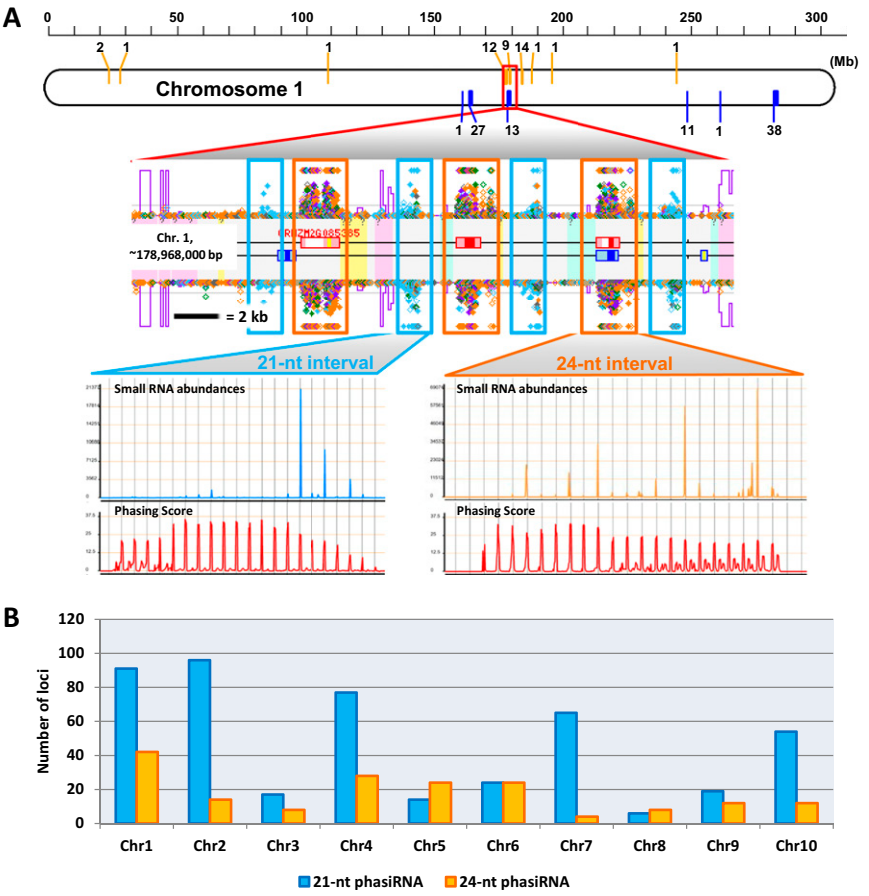

Fig. S1. Distribution of 21-*PHAS* and 24-*PHAS* loci within part of chromosome 1 and across the maize genome. (*A*) Example of one region on chromosome 1 that contains clusters of both 21- and 24-*PHAS* loci. In the *Middle* is a screenshot from our small RNA web browser: 21-nt sRNAs are indicated as light-blue spots, 22-nt sRNAs are indicated as green spots, and 24-nt sRNAs are indicated as orange spots, with other colors representing other sizes. Large, light blue rectangles highlight the 21-nt premeiotic phasiRNA loci and orange rectangles mark the 24-nt meiotic phasiRNA loci. Small blue boxes (on the *Bottom* strand) or red boxes (on the *Top* strand) are annotated genes. Purple lines indicate a k-mer frequency of the genome as an indication for repetitiveness; yellow, pink, or orange shading indicates DNA transposons, retrotransposons, or inverted repeats, respectively. (*B*) Count of 21- (blue) and 24- (orange) *PHAS* loci on each maize chromosome.

Fig. S2. Size distribution of phasiRNAs and their hits or repetitiveness in the maize genome. (*A*) Small RNAs from either the 21-nt or 24-nt phasiRNA generating loci in all 11 libraries (replication one) are combined and plotted for their size distribution. (*B*) Distribution of the number of perfect genome matches (hits) for 21-nt and 24-nt phasiRNAs, with the majority of phasiRNAs matching to only one position on the genome.

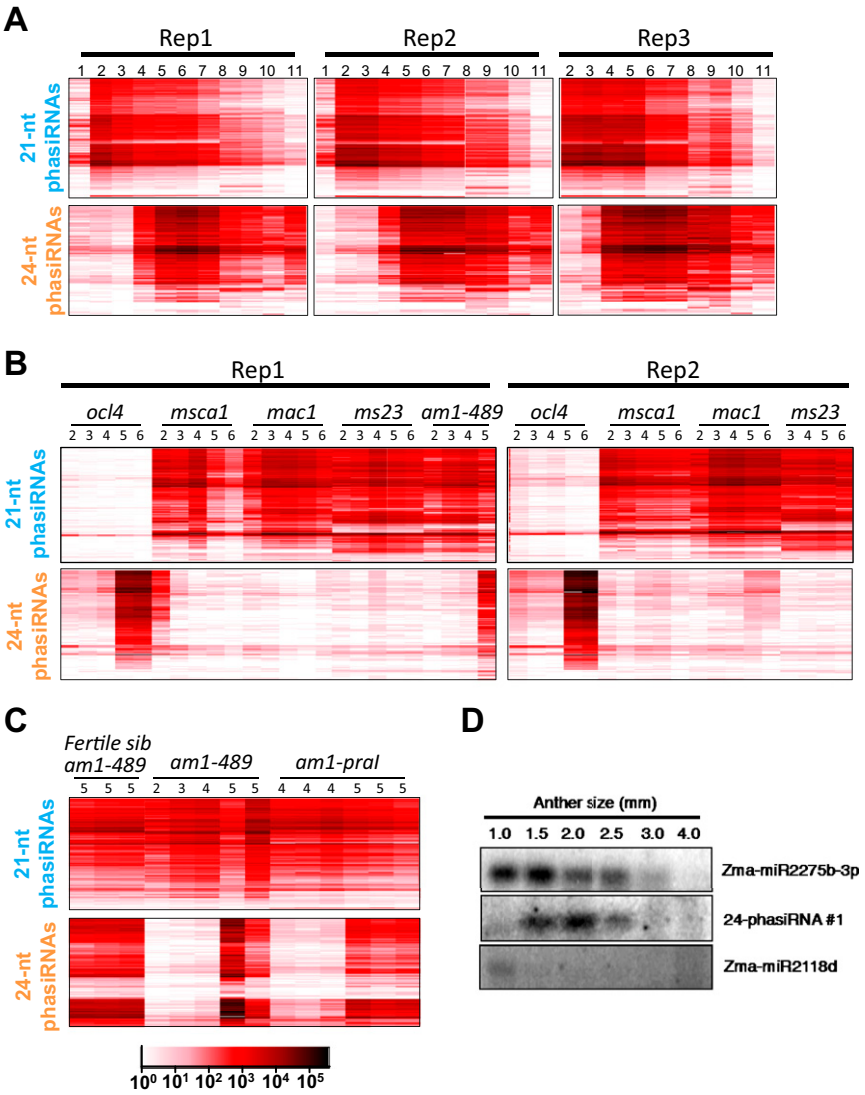

Fig. S3. Characterization of phasiRNA dynamics by small RNA sequencing and blotting. (*A*) PhasiRNA abundances are highly reproducible across biological replicates. Three biological replicates of phasiRNAs in fertile anthers, measured by small RNA sequencing at 11 stages. These data show a consistent trend of premeiotic and meiotic phasiRNAs. Only two replicates were used for the 0.2-mm anther because of the difficulty in obtaining tissue. The column numbers represent the 11 sampled stages, for example: 1 represents "0.2 mm" and 2 represents "0.4 mm", etc. (*B*) Two biological replicates of *ocl4*, *msca1*, *mac1*, and *ms23* anthers, each at five developmental stages, measured by small RNA sequencing for production of premeiotic phasiRNAs (*A*) and meiotic phasiRNAs (*B*). *TAS3*-derived ta-siRNAs and TE-derived siRNAs (*C*) are shown as control sRNA. More replicates of different *am1* alleles are shown in *C*. (*C*) *ameiotic1-489* and *ameiotic1-pral* have normal production of both premeiotic and meiotic phasiRNAs. *am1* mutant plants were obtained in families segregating 1:1 for *am1* homozygotes and *am1*/+ heterozygous fertile siblings; the fertile siblings of the *am1-489* allele family were also analyzed. (*D*) Splinted-ligation–based detection of miRNAs and phasiRNAs. (*Top*) The probe Zma-miR2275b-3p is a single member of the miR2275 family. (*Middle*) A high abundance meiotic phasiRNA was selected (see the sequence in Dataset S7). (*Bottom*) Zma-miR2118d is a single member of the miR2118 family. The experiment measuring a premeiotic phasiRNA gave no signal and thus is not shown. Ten micrograms of total RNA was used as input for each individual lane.

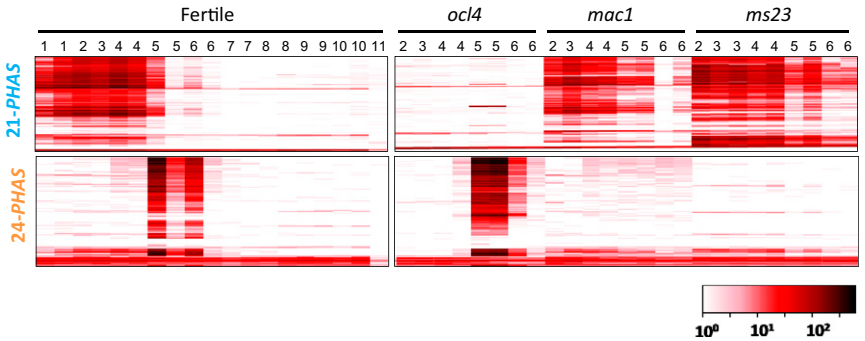

Fig. S4. Heat map of 21-*PHAS* and 24-*PHAS* precursors measured by RNA-seq in fertile anthers and mutants. Anther stages are indicted by the same numbering system as in Fig. S3. The numbers under the genotype indicate biological replicates. In fertile anthers, 21-*PHAS* transcripts peak from 0.4 mm to 0.7 mm and 24-*PHAS* transcripts peak from 1.5 mm to 2.0 mm.

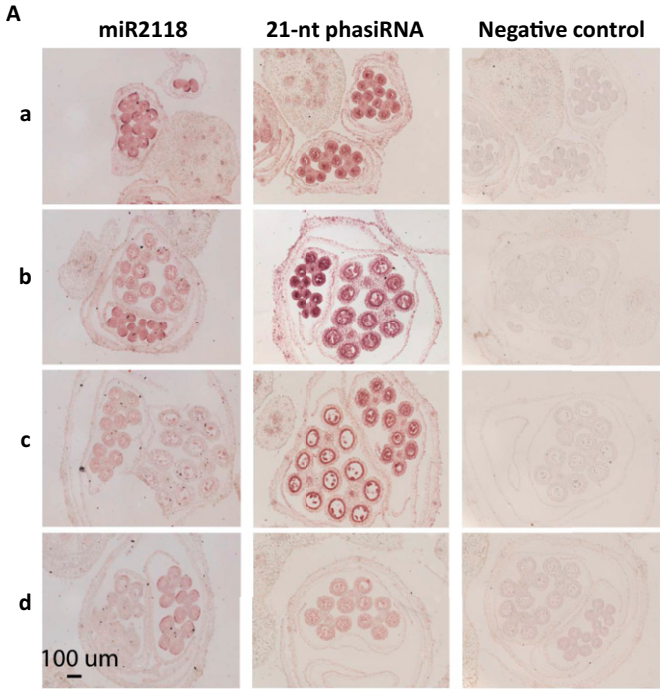

Fig. S5. (Continued)

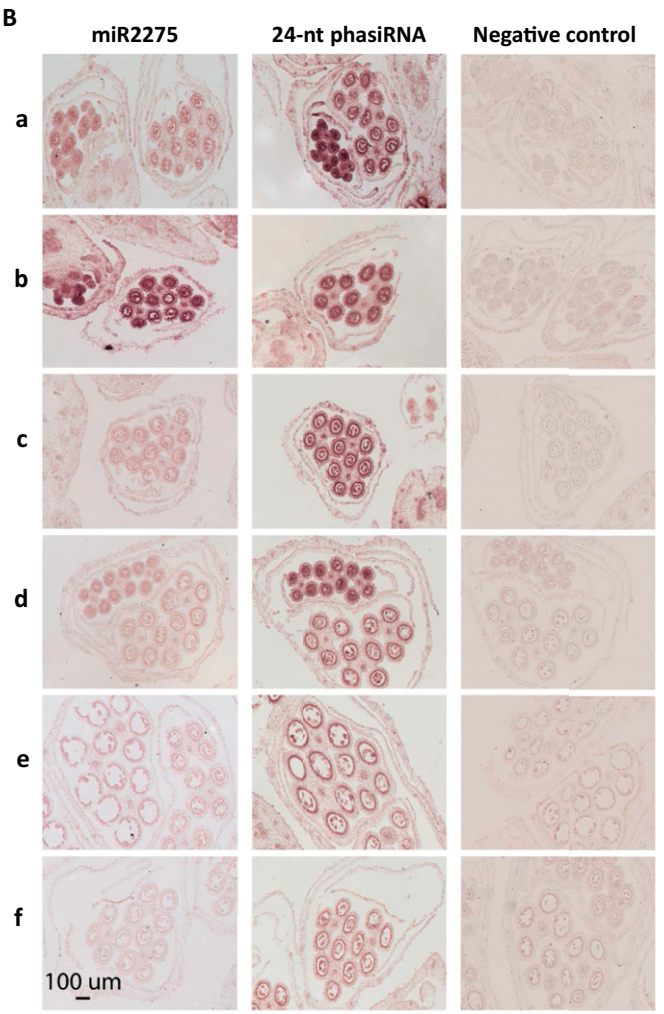

Fig. S5. (Continued)

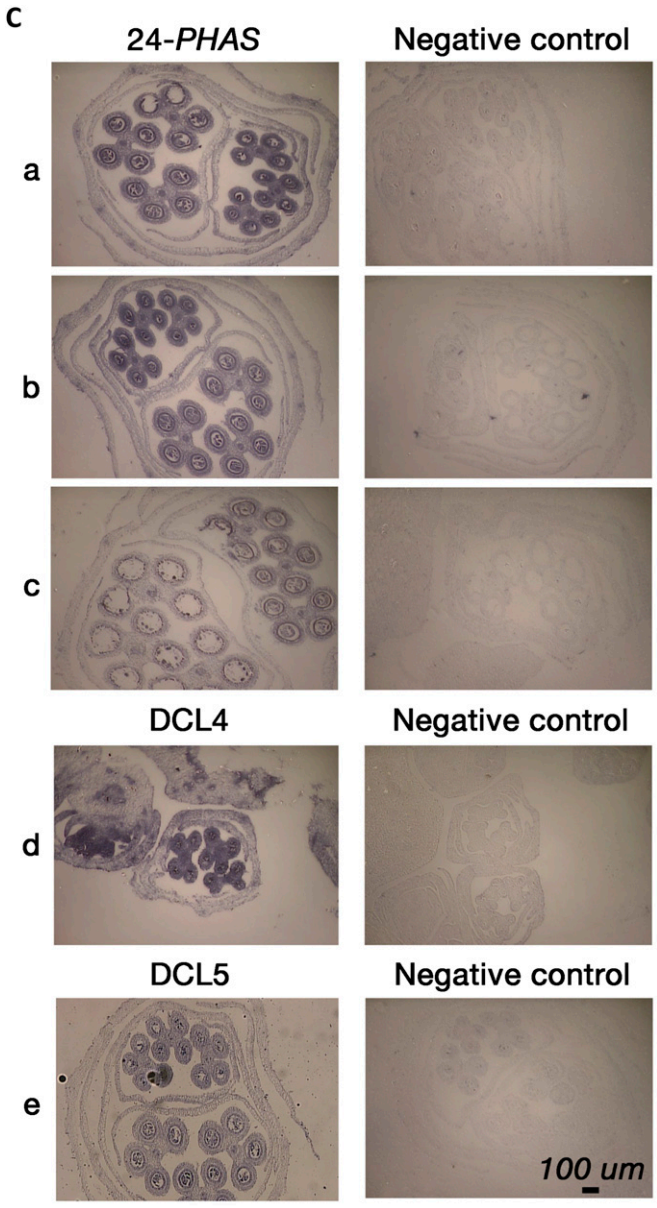

Fig. S5. Localization of phasiRNA pathway components by sRNA and mRNA in situ hybridization. (*A*) Localization of miR2118 and a premeiotic phasiRNA in maize anthers. Each maize spikelet contains two florets, and each of these contains three anthers. The upper floret anthers are about 1–2 d more advanced developmentally than the lower floret anthers in the same spikelet. In situ hybridizations were performed using anthers of (*a*) 0.5 mm, (*b*) 0.4 mm (small anthers) and 1.0 mm (larger anthers), (*c*) 1.0 mm (small anthers) and 2.0 mm (larger anthers), and (*d*) 0.7 mm (small anthers) and 1.5 mm (larger anthers). Anther sizes were estimated based on the organization of the cell layers. The negative control was a randomized sequence. Probe sequences are listed in Dataset S7. (*B*) Localization of miR2275 and a meiotic phasiRNA in maize anthers. In situ hybridizations were performed using anthers of (*a*) 0.4 mm (small anthers) and 1.0 mm (larger anthers), (*b*) 0.8 mm, (*c*) 1.0 mm, (*d*) 0.7 mm (small anthers) and 1.5 mm (larger anthers), (*e*) 1.0 mm (small anthers) and 2.0 mm (larger anthers), and (*f*) 1.6 mm. Anther sizes were estimated based on the organization of the cell layers. The negative control was a randomized sequence. Probe sequences are listed in Dataset S7. (*C*) Localization of 24-*PHAS*, DCL4, and DCL5 in maize anthers by mRNA in situ hybridization. In situ hybridizations were performed for analysis of mRNAs precursors and Dicer transcripts, using anthers of (*a*) 0.8 mm (small anther) and 1.5 mm (larger anther), (*b*) 1.0 mm (small anthers) and 1.5 mm (larger anthers), (*c*) 1.5 mm (small anthers) and 2.5 mm (larger anthers), (*d*) 0.4 mm, and (*e*) 1.5 mm (small anthers) and 2.5 mm (large anthers). Anther sizes were estimated based on the organization of the cell layers. For DCL4 and DCL5, sense probes were used as negative controls. For *PHAS* precursors, because transcripts are converted to double-stranded RNAs, both sense and antisense probes have strong signals. Therefore, we used a DIG-labeled antisense Neo RNA included in the DIG RNA Labeling kit for negative controls. Probe sequences are listed in Dataset S7. The 21-*PHAS* precursors are of low abundance and only detectable at 1.0-mm anther stages as shown in *B*, therefore time series in situ are not shown.

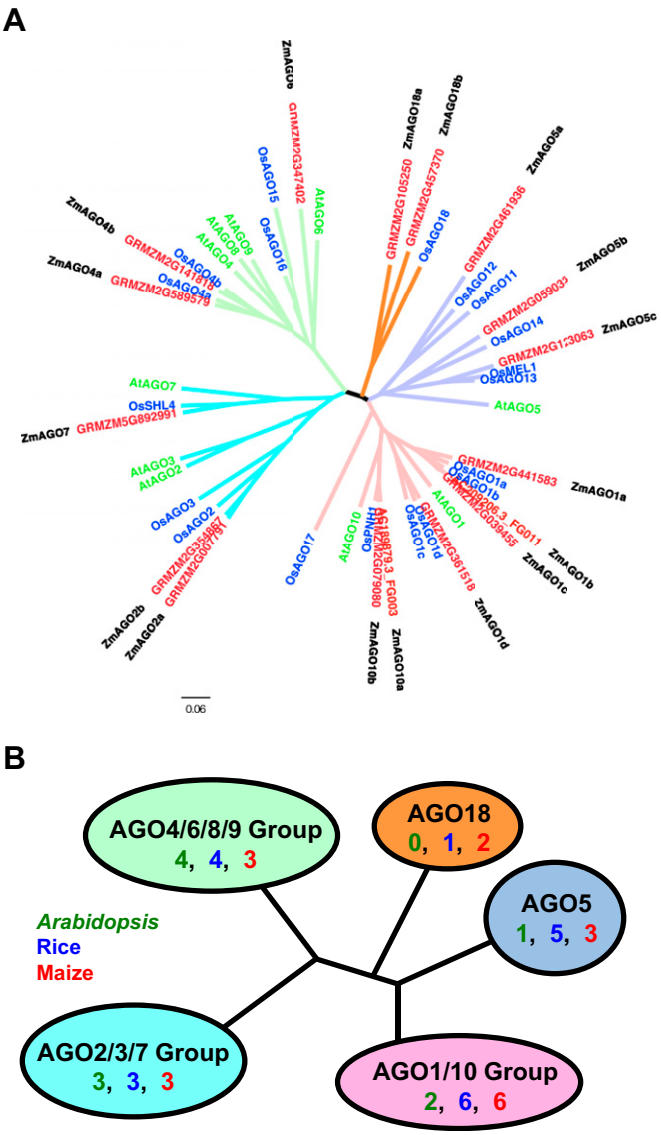

Fig. S6. Evolutionary relationship of AGOs in maize, rice, and *Arabidopsis*. (*A*) An unrooted phylogenetic tree of the AGO proteins. Green identifiers are from *Arabidopsis*, blue from rice, and red from maize. (*B*) Divergence of plant AGO families. Numbers of AGO proteins within a particular group are listed for each species, color coded as in *A*.

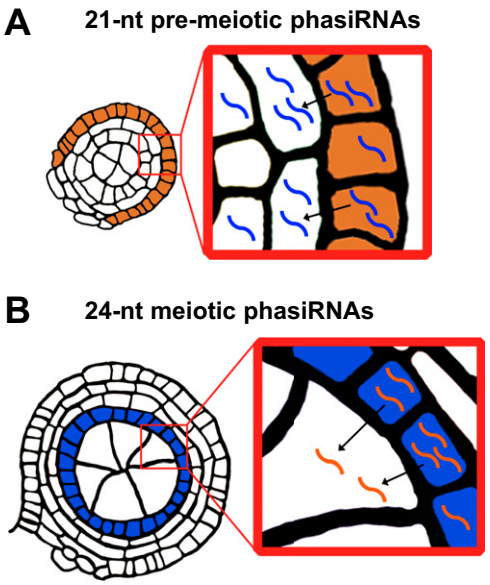

Fig. S7. Cartoon illustration of proposed movement of phasiRNAs. Premeiotic phasiRNAs are generated in the epidermis and transfer to the subepidermal cells (*A*), whereas meiotic phasiRNAs move from the tapetum to PMCs (*B*) to perform their functions.

Other Supporting Information Files

Dataset S1 (XLS)
Dataset S2 (XLSX)
Dataset S3 (XLSX)
Dataset S4 (XLSX)
Dataset S5 (XLSX)
Dataset S6 (XLSX)
Dataset S7 (XLSX)